Journal of Molecular Catalysis A: Chemical 310 (2009) 130–137

Contents lists available at ScienceDirect

Journal of Molecular Catalysis A: Chemical

journal homepage: www.elsevier.com/locate/molcata

Effect of variations in pore structure and acidity of alkali treated ZSM-5 on the isomerization performance

Yue-Qin Song[a], Yan-Long Feng[a], Feng Liu[a], Cheng-Lin Kang[a], Xiao-Long Zhou[a,*], Long-Ya Xu[b], Guo-Xian Yu[c]

[a] Petroleum Processing Research Center, East China University of Science and Technology, Shanghai 200237, PR China
[b] State Key Laboratory of Catalysis, Dalian Institute of Chemical Physics, Dalian, Liaoning 116023, PR China
[c] School of Chemistry and Environment Engineering, Jianghan University, Wuhan, Hubei 430056, PR China

ARTICLE INFO

Article history:
Received 19 September 2008
Received in revised form 20 May 2009
Accepted 5 June 2009
Available online 16 June 2009

Keywords:
Alkali treatment
Hydro-isomerization
Acidity
Mesopore
Pt/ZSM-5

ABSTRACT

A series of alkali treated ZSM-5 samples were prepared and the effects of the alkali treatment conditions on the n-hexane isomerization performance of Pt/ZSM-5 were investigated. The characterization by XRD, N_2-adsorption, XRF, NH_3-TPD, Py-IR and NMR revealed that alkali treatment conditions had the effects on the crystallinity, textural property, Si/Al ratio and acidity of ZSM-5. Mild alkali treatment led to the reduction of the strong acid sites and did not distinctly change the pore structure, whereas severe alkali treatment resulted in the creation of the stronger acid sites and new mesopores. The correlation of the acidity and pore structure and isomerization behavior was established. It was proposed that the conversion of n-hexane was dependent on the amount of strong acid sites and irrelevant to the properties of acid sites and the pore structure. However, the selectivity for iso-hexanes was irrelevant to both the acidity and pore structure. The relative amount of dimethylbutanes (DMB) and methylpentanes (MP) in isomers was related not only to the pore structure, but to the acidity of ZSM-5. The suitable alkali treatment condition facilitated the high yield of isomers and the formation of more DMB.

1. Introduction

Iso-alkanes, especially multibranched alkanes possess high octane number and are desired components of gasoline pool. Therefore, the hydro-isomerization of n-alkanes to isoalkanes is of practical importance. Hydro-isomerizaiton of n-paraffin often requires bifunctional catalysts containing acid sites and metal sites [1–4]. Zeolites, especially microporous zeolites have many advantages, such as high specific surface area, high thermal stability and considerably strong acid sites. Accordingly, n-paraffin hydro-isomerization over Pt/zeolite catalysts attracted much attention [5–19]. Some investigations have demonstrated that the acidity and pore structure of zeolite would influence the n-alkanes isomerization behavior over zeolite-supported Pt catalyst [8–14]. The acid-leaching, steaming and the ammonium hexafluorosilicate treatment of zeolite were conventional methods for modifying the pore structure and acidity of zeolites. Moreover, these treatment methods for improving the isomerization performance of Pt/zeolite have been widely studied. van Donk and Tromp et al. [15,16,20] enhanced the isomerization activity of mordenite by acid-dealumination. An investigation from van Bokhoven et al. [18] indicated that the isomerization activity was enhanced over steamed mordenite. Additionally, Viswanadham et al. [21] found that the steaming of mordenite following by acid-leaching could also improve the isomerization activity of Pt/mordenite. However, Corma et al. [22] treated Beta zeolite by different methods and found that the combination of extra-framework Al and the OH groups of framework Al were favorable to the enhancement in the isomerization activity. A study by Baeck and Lee [23] revealed that steaming treatment at high temperature reduced the activity in isomerization of n-butene to isobutene over Mg-ZSM-22, while the treatment with diluted nitric acid improved the catalytic activity.

As a new method for modifying zeolite, alkali treatment has received more and more attention, especially in the material field [24–31]. Alkali treatment of zeolites is different from acid-leaching, steaming treatment and ammonium hexafluorosilicate treatment in that the former mainly led to desilication and the latter mainly led to dealumination [25,26,28–31]. Several reports pointed out that the slight dealumination also would occur in alkali treatment [29,31,32]. To our knowledge, there have only been few

* Corresponding author at: Research Institution of Petroleum Processing, East China University of Science and Technology, No 130, Meilong Road, Shanghai 200237, PR China. Tel.: +86 21 64253049; fax: +86 21 64253049.
E-mail addresses: yqsong@mail.tsinghua.edu.cn (Y.-Q. Song), 83889629@163.com (Y.-L. Feng), bt4012006@163.com (F. Liu), cortny@mail.ecust.edu.cn (C.-L. Kang), xiaolong@ecust.edu.cn (X.-L. Zhou), lyxu@dicp.ac.cn (L.-Y. Xu), guoxianyu828@yahoo.com.cn (G.-X. Yu).

1381-1169/$ – see front matter © 2009 Elsevier B.V. All rights reserved.
doi:10.1016/j.molcata.2009.06.006

Table 1
SiO_2/Al_2O_3 molar ratio and textural properties of ZSM-5 samples under various alkali treatment conditions.

Sample	ZSM-5(P)	ZSM-5(AT1)	ZSM-5(AT2)	ZSM-5(AT3)	AT3-C	ZSM-5(AT4)
NaOH solution (mol/l)	–	0.05	0.05	0.1		0.3
Treating time (h)		2	8	8		8
Molar ratio of Si/Al_2	55.0	48.6	53.5	48	50.9	30.0
S_{BET} (m^2/g)[a]	331	350		391	401	406
ΔS_{ext} (m^2/g)[b]		15		50	60	62
Vol_{micro} (cm^3/g)[c]	0.107	0.113		0.113	0.112	0.113
Vol_{meso} (cm^3/g)[d]	0.09	0.12		0.21	0.32	0.46

[a] Specific surface area of BET.
[b] Increment of external specific surface area before and after alkali treatment.
[c] Volume of micropres.
[d] Volume of mesopores.

investigations about the application of the alkali-treatment of zeolite in catalytic reaction. Lietz and Ogura et al. [26,28] reported that the propane aromatization activity and cumene cracking activity were drastically enhanced on alkaline-treated ZSM-5. In addition, the alkali treatment of ZSM-5 led to an enhancement in the stability in butene and methane aromatization [29,33]. Li et al. [34] recently reported that the alkali-treatment of ZSM-5 led to a considerable enhancement both in the 1-hexene aromatization and isomerization activity. However, little work has been carried out to investigate the effect of alkali treatment of zeolite on n-alkane isomerization behavior.

The purpose of the present work is to investigate the variations in the acidity and pore structure of ZSM-5 resulting from alkali treatment and their effects on the n-hexane isomerization behavior. We also expected to improve the isomerization activity of Pt/ZSM-5 by the alkali treatment under appropriate conditions.

2. Experimental

2.1. Catalyst preparation

Na-form ZSM-5 zeolite powder with a SiO_2/Al_2O_3 molar ratio of 55 (provided by Fushun Catalyst Plant, China) was calcined in flowing air at 550 °C for 5 h to remove the hexanediamine template and denoted as ZSM-5(P).

2.1.1. Alkali treatment

The ZSM-5(P) sample was treated with different concentration of NaOH solution and different times, as listed in Table 1. The treatment procedure was as follows. A 2000 ml of NaOH solution was heated to 70 °C in a polyethylene flask. Then, 35 g of the calcined sample was added to the heated aqueous NaOH with the mixture stirred at the temperature for given time. The slurry was then cooled down immediately using an ice-water bath, filtered and washed thoroughly till the pH of the filtration solution decreased to 7, followed by drying at 120 °C for 10 h. The labels of the obtained samples are listed in Table 1.

2.1.2. Acid treatment

Part of the ZSM-5(AT3) sample was used for the further acid treatment. The procedure of the acid treatment was as follows. ZSM-5(AT3) was first converted into H-form by exchanging with ammonium nitrate solution and subsequently calcination at 550 °C. Then, 200 ml of 0.1 M nitrate acid was heated to 70 °C in a flask and 5 g of the HZSM-5(AT3) sample was put into the 0.1 M nitrate acid solution preheated to 70 °C and kept at this temperature for 24 h with stirring. After that, the slurry was cooled down, washed and dried and the resulting sample was designated as ZSM-5(AT3)-C. All the treated samples, together with ZSM-5(P), were extruded with alumina as binder (30 wt%) to obtain the extrudates. After calcination at 500 °C for 2 h, the extrudates were treated with 0.8 M ammonium nitrate solution and washed with deionized water at 80 °C repeatedly, to convert into the NH_4-form. After drying, the samples in the NH_4-form were calcined at 520 °C to be converted into the H-form.

2.1.3. Pt loading

The Pt/ZSM-5 catalysts were prepared by impregnation with H_2PtCl_6 solution. The extrudate was added to H_2PtCl_6 solution with the given concentration to ascertain 0.5% loading of Pt. Then, the sample loaded with Pt was kept at room temperature for 24 h, dried at 110 °C for 10 h and calcined at 500 °C for 3 h to obtain 0.5%Pt/ZSM-5 catalyst. The catalysts were crushed and sieved to 60–80 mesh particles before they were loaded into the reactor.

2.2. Catalytic testing for n-hexane isomerization

The isomerization reaction of n-hexane (AR) was performed in a continuous flow fixed-bed stainless steel reactor (i.d. = 5 mm). Catalyst of 1 g (30–50 mesh) was loaded in the reactor and pretreated in drying air flow at 400 °C for 3 h to remove the impurity absorbed on the surface of catalyst. Then, the catalyst bed was cooled down to 280 °C and reduced at the temperature in a flow of hydrogen (15 ml/min) for 2 h. Finally, the temperature of the catalyst bed decreased to given temperature and hydrogen and n-hexane were simultaneously introduced into the reactor. The molar ratio of H_2 to n-hexane was 30, reaction pressure was 2 MPa and weight hourly space velocity (WHSV) was 1 h^{-1}. The flow rate of hexane and hydrogen was controlled with a double column pump and a mass flow meter, respectively. The products were heated and then analyzed on-line by GC-920 with an OV-101 capillary column, connected with an FID.

2.3. Catalyst characterization

X-ray powder diffraction (XRD) was carried out on a Philips MagiX X-ray diffractometer, using Cu Kα1 radiation at room temperature and instrumental settings of 40 kV and 40 mA. The scanning rate was 10°/min and scanning range was from 10° to 70°.

N_2 adsorption and desorption experiments were performed in liquid nitrogen at −196 °C on the NOVA 4000 gas adsorption analyzer (Quantachrome Corp.). Each sample was evacuated at 350 °C for 10 h before N_2 adsorption. The total surface area was calculated according to the BET isothermal equation, and the micropore volume and external surface area were evaluated by the *t*-plot method. Mesopore distribution was obtained according to the BJH method.

NH_3-temperature programmed desorption (NH_3-TPD) was carried out at a home-made equipment. The sample (0.14 g) was loaded into a stainless steel U-shaped microreactor (i.d. = 5 mm) and pretreated at 600 °C for 0.5 h in flowing He. After the pretreatment, the sample was cooled down to 150 °C and was exposed to NH_3 atmosphere. As the catalyst is saturated with the adsorbed NH_3, He was

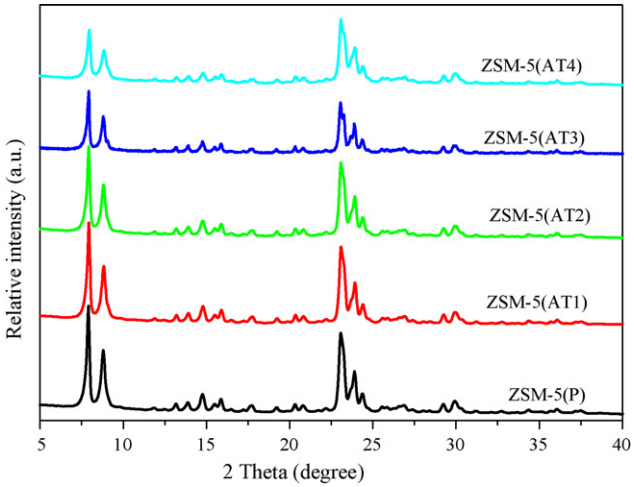

Fig. 1. XRD patterns of the ZSM-5 samples before and after alkali treatment.

used as carrier to remove NH_3 physically adsorbed until the baseline was stabilized. NH_3-TPD was then carried out in a constant flow of He (20 ml/min) from 150 to 650 °C at a heating rate of 18 °C/min. The concentration of ammonia in the exit gas was monitored continuously by a gas chromatograph (Shimazu 8A) equipped with a TCD.

Multinuclear MAS NMR experiments were carried out at 9.4 T on a Bruker DRX-400 spectrometer using 4-mm ZrO_2 rotors. ^{27}Al MAS NMR spectra were recorded at 104.3 MHz and the sample was spun at 4 kHz. 1% $Al(H_2O)_6^{3+}$ was used as reference of chemical shifts.

Pyridine adsorption infra-red (Py-IR) was carried out on an EQUIOX 55 Fourier transform infrared spectrometer (Bruker Corp.). Self-supporting wafers of the samples (ca. 10 g, 10 mm diameter) were loaded on the IR cell. The wafer was evacuated 500 °C and then cooled down to room temperature for the record of background spectra. The wafer was saturated with pyridine, evacuated at 150 °C for 0.5 h and then again cooled to room temperature. FTIR spectra were recorded at a spectra resolution of 2 cm^{-1} with the subtraction of the sample background. Subsequently, the wafer was evacuated at 350 °C for 0.5 h and then again cooled to room temperature and the recording of FTIR spectra followed the above procedure.

Scanning electron microscopy (SEM) was conducted on KYKY100B to investigate the morphology of samples before and after the alkali-treatment.

3. Results and discussion

3.1. Crystal structure and morphology

Fig. 1 gives the XRD patterns of ZSM-5 before and after alkali treatment. It can be seen that the intrinsic crystalline structure of ZSM-5 remained and no new phase emerged after the alkali treatment. The concentration of alkali influenced significantly the relative crystallinity of ZSM-5. The relative crystallinity of ZSM-5 hardly changed when the alkali concentration was lower than 0.05 mol/l. It decreased distinctly when the alkali concentration was beyond 0.05 mol/l, implying that the microstructure was destroyed. Meanwhile, the destruction also led to the changes in the morphology of crystals, as shown in Fig. 2. The morphology of ZSM-5 was changed after the alkali treatment to some extent. The small particles existed in ZSM-5 (P) (Fig. 2A), which may be related to

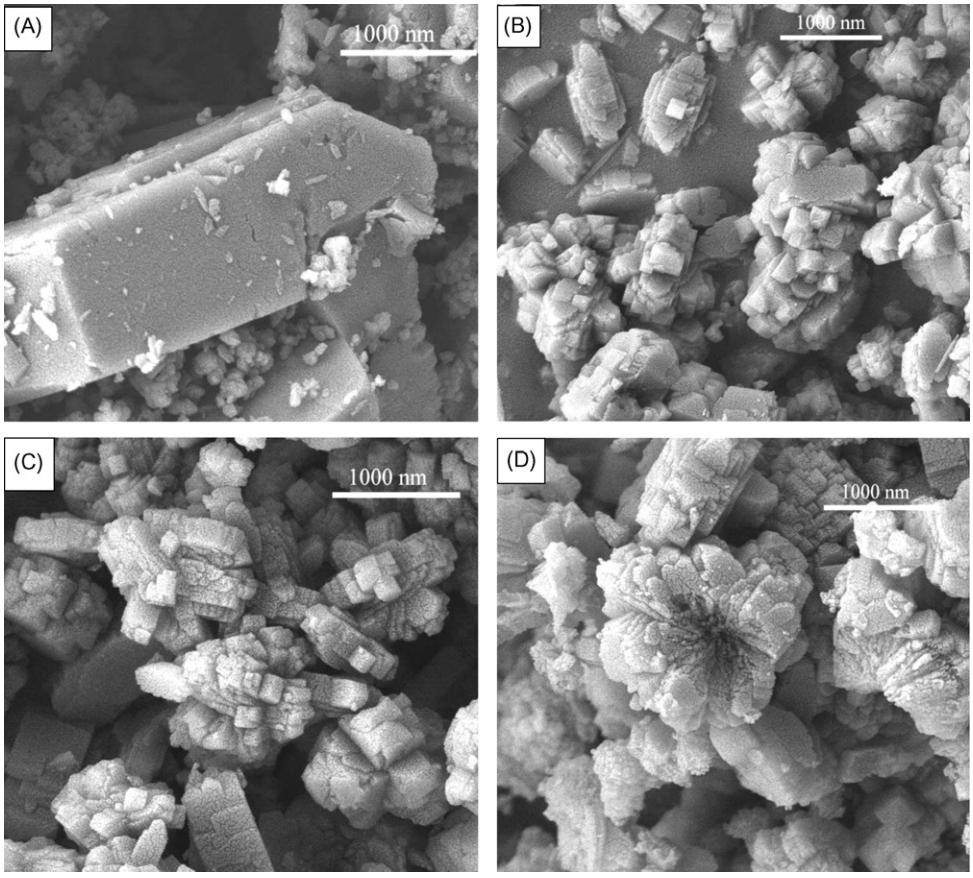

Fig. 2. SEM of ZSM-5 under the various alkali-treatment conditions.

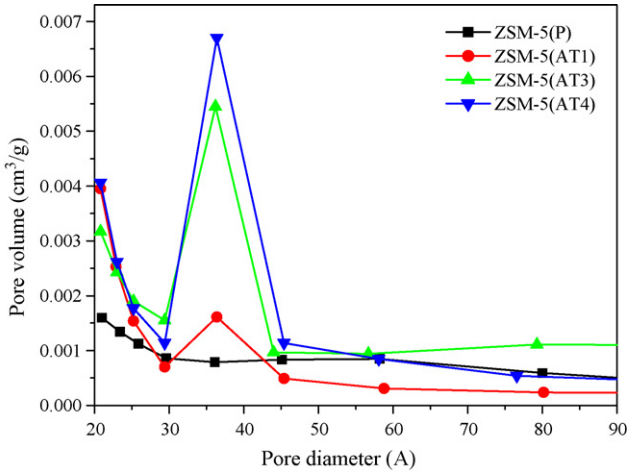

Fig. 3. Pore diameter distribution of mesopores in ZSM-5(P) and ZSM-5(AT) samples.

the amorphous silica species formed in the hydrothermal synthesis. After the mild alkali treatment, the small particles disappeared (Fig. 2B). Meanwhile, the molar ratio of Si/Al decreased distinctly when the alkali treatment condition was very mild. This further confirmed that small particles should be amorphous silica species. The coffin structure was almost lost and there appeared more edges and planes (Fig. 2B and C) with the increase in the alkali concentration. Further increasing in the concentration of NaOH led to the disappearance of the newly formed planes and edges (Fig. 2D) and the surface of the particles also became rough. In addition, the particles became small upon the alkali treatment.

3.2. Textural properties of ZSM-5

The influence of the alkali treatment on the textural properties of ZSM-5 was studied by N_2 adsorption–desorption measurement at −196 °C, and the results are listed in Table 1. An increment in the external surface area was only 15 m^2/g after the mild treatment, whilst the value increased significantly from 15 m^2/g of ZSM-5(AT1) to 47 m^2/g of ZSM-5(AT3) and 62 m^2/g of ZSM-5(AT4), indicative of the creation of mesopores, as evidenced by BJH pore diameter distributions (in Fig. 3). The volume of the mesopores increased with the alkali concentration. However, the change in the micropores was not obvious after alkali treatment. In order to further confirm the creation of mesopores in the alkali treatment, N_2 adsorption isotherms of different samples were also provided, as shown in Fig. 4. The untreated sample P represented I-type isotherm with a plateau at higher relative pressure, which was typical for microporous materials. However, with the alkali treatment processing there appeared notable hysteresis in the relative pressure range of 0.4–1.0. Moreover, the hysteresis became pronounced at high pressure with increasing severity of the alkali treatment. This further confirmed the above proposal that the alkali treatment of ZSM-5 led to the creation mesopores and the mesopores became more abundant with increasing severity of alkali treatment. These new mesopores may result from the gap between particles or be related to the rough surface and the decreased size in the particles. The changes in the pore structure after the alkali treatment may have an effect on the isomerization performance of Pt/ZSM-5 although the creation mechanism of mesopores was in debate [35–40].

3.3. Si/Al ratio of ZSM-5

Since the alkali treatment of zeolite would lead to a preferential desilication [24–30] the SiO_2/Al_2O_3 ratio in zeolite should change in the alkali treatment. Table 1 provides the variations of SiO_2/Al_2O_3 ratio with the treatment conditions. Noting that the alkali treatment led to a decrease in the SiO_2/Al_2O_3 molar ratio, and that both the treatment time and alkali concentration had an important influence on the ratio. At the same treatment time of 8 h, the ratio decreased gradually from 53.5 of ZSM-5(AT2) for 0.05 M NaOH solution to 48 of ZSM-5(AT3) for 0.1 M NaOH and 30 of ZSM-5(AT4) for 0.3 M NaOH. It seemed that the more severe the alkali treatment conditions were, the higher the degree of desilication. Besides the NaOH concentration, the treatment time would influence the SiO_2/Al_2O_3 ratio. Unexpectedly, the ratio of ZSM-5(AT1) treated for 2 h with 0.05 M NaOH was 48.6, much lower than 53.5 of ZSM-5(AT2) treated for 8 h. An investigation from Ogura et al. [28] showed that desilication of zeolite was accompanied by the occurrence of dealumination. Additionally, a recent report from Li et al. [34] suggested that the dissolved Si in NaOH aqueous solution may deposit on ZSM-5 as amorphous Si species (backward reaction). Both the dealumination and the deposit of Si species in solution may be the main factors leading to the increase in the ratio of SiO_2/Al_2O_3 with the prolonged treatment time.

3.4. ^{27}Al NMR

In order to further clarify whether framework dealumination occurred during alkali treatment, ^{27}Al NMR of the samples was conducted and the results are shown in Fig. 5. For ZSM-5(P), there appeared a strong band at 55 ppm and a weak band at −2 ppm, which was associated with framework Al (Al_{FW}) and extra-framework Al (Al_{EF}), respectively. The measurement showed that there existed a small amount of Al_{EF} in ZSM-5(P) except for large amount of Al_{FW}. After the mild alkali treatment with 0.05 M NaOH for 2 h, the weak band at −2 ppm disappeared, indicative of the removal of Al_{EF} in ZSM-5(P). Noticeably, the band at −2 ppm reappeared and became stronger with the increasing alkali concentration. This indicated that partial Al was removed from the matrix of ZSM-5 and transformed into Al_{EF} possibly because more framework Si was removed and the Al_{FW} attached to framework Si became instable and easy to remove. The above results indicated that the alkali treatment led to the change in the SiO_2/Al_2O_3 ratio and possibly provoked the change in the acidity of ZSM-5 to further influence the catalytic performance.

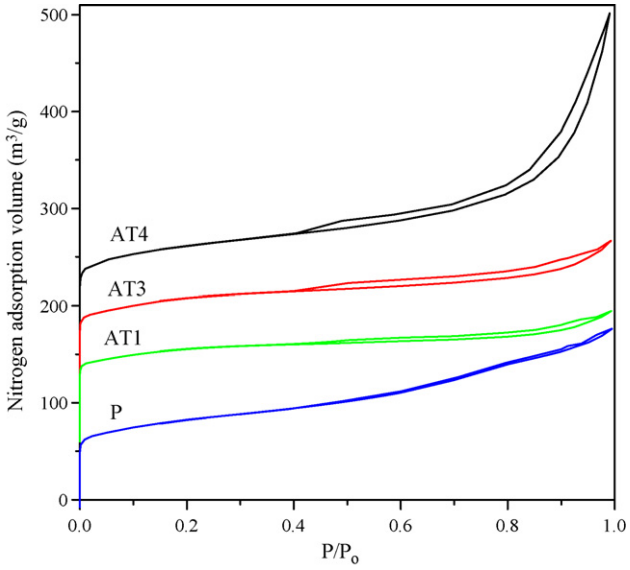

Fig. 4. N_2 adsorption isotherms of alkali-treated ZSM-5 under various concentrations.

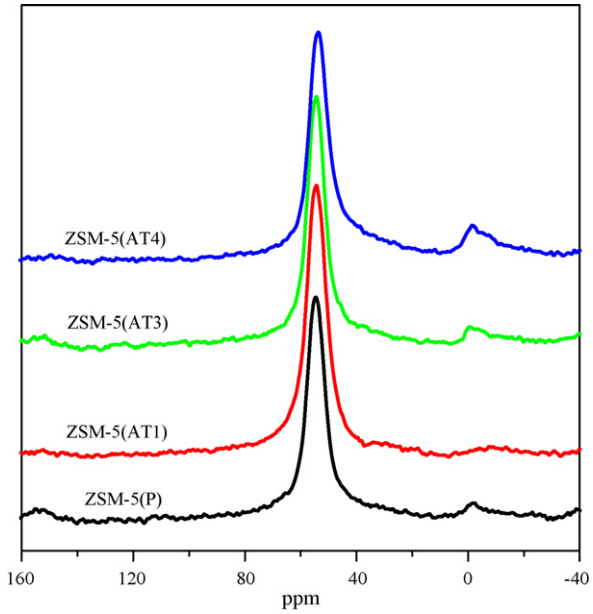

Fig. 5. ^{27}Al NMR of ZSM-5 before and after alkali treatment.

3.5. Acidity of ZSM-5

The acidity of ZSM-5 was studied by NH_3-TPD and results are shown in Fig. 6. In the NH_3-TPD curve of untreated sample ZSM-5(P), there emerged two distinct NH_3 desorption peaks at about 270 and 470 °C, corresponding to the weak and the strong acid sites, respectively. It was seen that the strong acid sites decreased obviously after the mild alkali treatment and that almost no change in the weak acid sites occurred. The reduction of the strong acid sites may be related to the removal of Al_{EF} in ZSM-5(P) as confirmed by the ^{27}Al NMR spectra. As the severity of the alkali treatment condition increased, the total acid sites, including both the strong and weak acid sites, distinctly increased. As described above, the severe alkali treatment led to a significant reduction in the molar ratio of Si/Al. Hence, the increase in the total acid sites was closely related to the desilication. In addition, a new and distinct NH_3 desorption peak appeared at a high temperature of 600 °C for ZSM-5(AT3) and ZSM-5(AT4), indicating the creation of the stronger acid sites. Combined with the finding from ^{27}Al NMR (Fig. 5) that Al_{EF} were present in ZSM-5(AT3) and ZSM-5(AT4), it was reasonable to conclude that the stronger acid sites on ZSM-5(AT3) and ZSM-5(AT4) mainly originated from Al_{EF} [32,41,42].

For the sake of further confirming the above proposal that the new stronger acid sites derived from Al_{EF}, ZSM-5(AT3) was further treated by diluted nitric acid at 70 °C to remove Al_{EF} according to the reported results [43] to obtain ZSM-5(AT3)-C sample. The molar ratio of Si/Al of the acid treated sample ZSM-5(AT3)-C was distinctly higher than that of the sample ZSM-5(AT3) untreated with acid, as shown in Table 1, indicative of the removal of Al in the acid treatment. Moreover, the new stronger acid sites ZSM-5(AT3) after acid treatment disappeared, as shown in Fig. 7. Hence, it was reasonable to conclude that the new stronger acid sites on ZSM-5(AT3) were from the Al_{EF} formed in the alkali treatment.

The variations of the acidic properties with alkali treatment conditions were further characterized by Py-IR at 150 and 350 °C, as shown in Fig. 8. The spectra at 150 and 350 °C represented the properties of the total and strong acid sites, respectively. The bands centering at ca. 1540 and 1450 cm^{-1} were related to the Brønsted acid sites and Lewis acid sites, respectively. For the properties of total acid sites, the mild treatment led to a distinct reduction in the Brønsted acid sites and no significant change in Lewis acid sites occurred (Fig. 8a). Combined with the results from ^{27}Al NMR, it could be concluded that the removal of Al_{EF} in ZSM-5(P) should be mainly responsible for the decrease in the Brønsted acid sites. In turn, this also indicated that the Al_{EF} could produce Brønsted acid sites. An obvious increase in the Lewis and Brønsted acid sites on the severely treated ZSM-5 was observed, indicating the increase in the total acid sites, in line with the results of NH_3-TPD. However, for the properties of the strong acid sites, the mild alkali treatment led to a decrease in the Brønsted acid sites and an increase in the Lewis acid sites (Fig. 8b). With the increase in the alkali concentration, the Brønsted acid sites increased and no distinct change occurred in the Lewis acid sites. As the alkali concentration further increased, both the Brønsted and Lewis acid sites continued to increase, while the increase in the latter was more obvious. The creation of more strong Lewis acid sites over ZSM-5(AT4) may be related to the presence of more Al_{EF} [44].

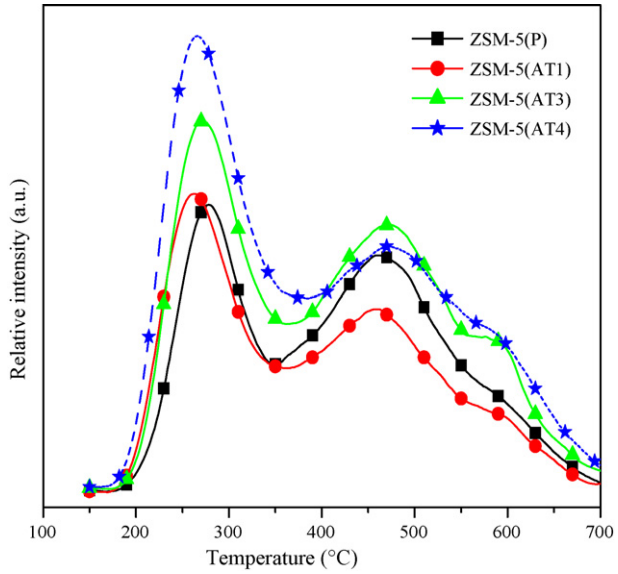

Fig. 6. NH_3-TPD profiles of ZSM-5(P) and ZSM-5(AT).

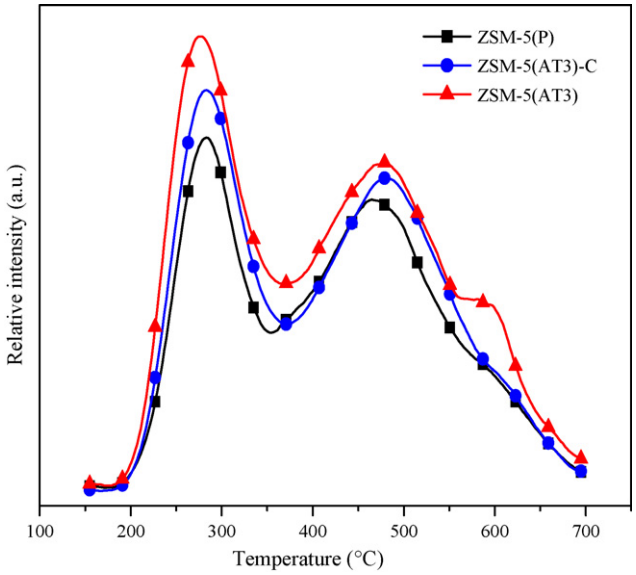

Fig. 7. NH_3-TPD profiles of ZSM-5(P) and ZSM-5(AT3)-C.

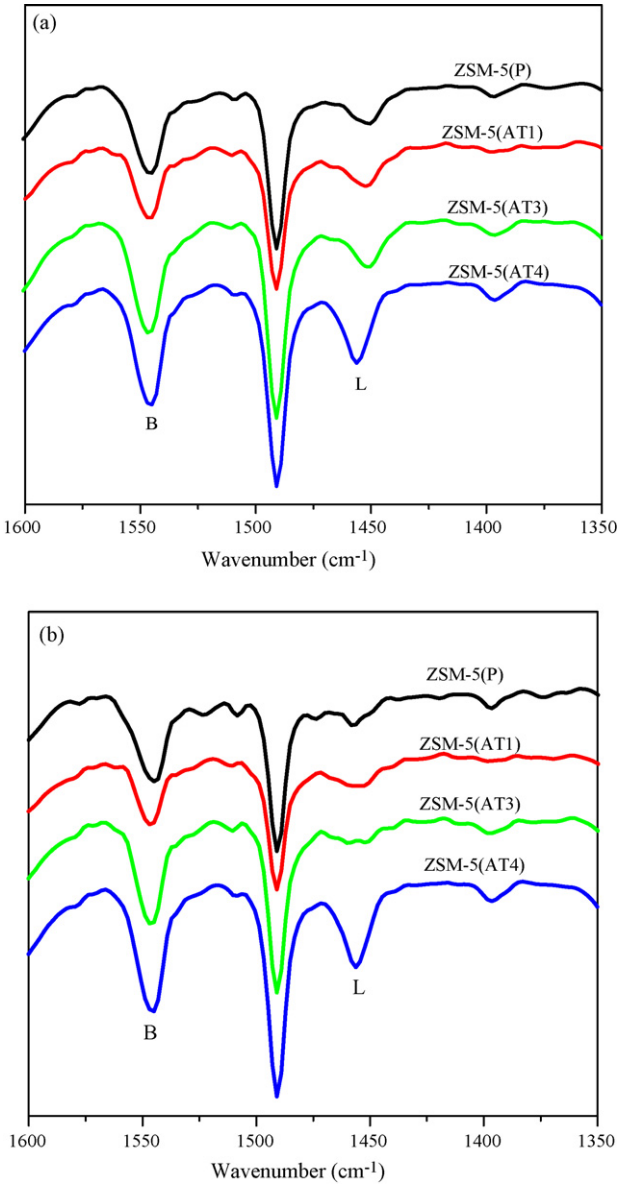

Fig. 8. Py-IR spectra of ZSM-5(P) and ZSM-5(AT).

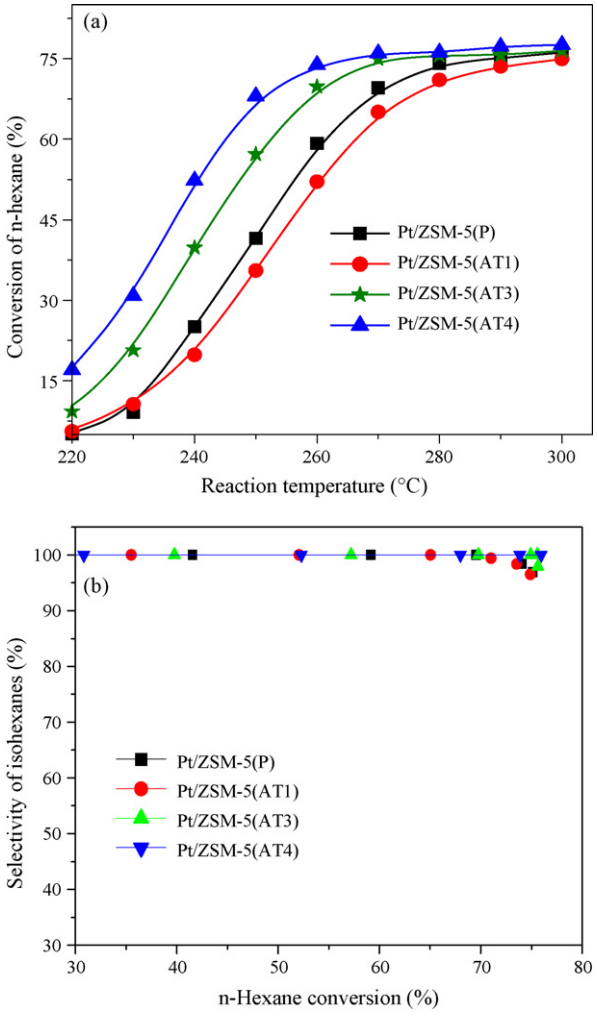

Fig. 9. Conversion of n-hexane and selectivity for isohexanes over Pt/ZSM-5(P) and Pt/ZSM-5(AT).

3.6. Isomerization performance of Pt/ZSM-5

The significant changes in the acidity and the pore structure of ZSM-5 resulting from the alkali treatment may influence the catalytic activity. Thus, the hydro-isomerization performance of Pt/ZSM-5 treated under different alkali conditions was investigated and the results are presented in Fig. 9. Obviously, the conversions of *n*-hexane over the different catalysts showed great difference (Fig. 9a). After the mild alkali treatment, the conversion showed a distinct decrease. In contrast, the severe alkali treatment led to a significant increase in *n*-hexane conversion. However, the selectivities for isohexanes over all the catalysts were close to each other at the same conversion of n-hexane (Fig. 9b). Meanwhile, it was noted that cracking reaction hardly occurred and the selectivity was close to 95% at the conversion lower than 70%. As the conversion increased up to 75%, only slight cracking occurred and the selectivities over the different catalysts were still higher than 95%. As for the distribution of isohexanes, the values over different catalysts exhibited great difference, as shown in Fig. 10. The ratio of DMB to MP in isohexanes over Pt/ZSM-5(AT1) was obviously lower than that over Pt/ZSM-5(P). However, the values over Pt/ZSM-5(AT3) and Pt/ZSM-5(AT4) were higher than the value over Pt/ZSM-5(P). The above results indicated that the alkali treatment of ZSM-5 had a great effect on the isomerization performance of Pt/ZSM-5. Moreover, the severe treatment not only could enhance the isomer-

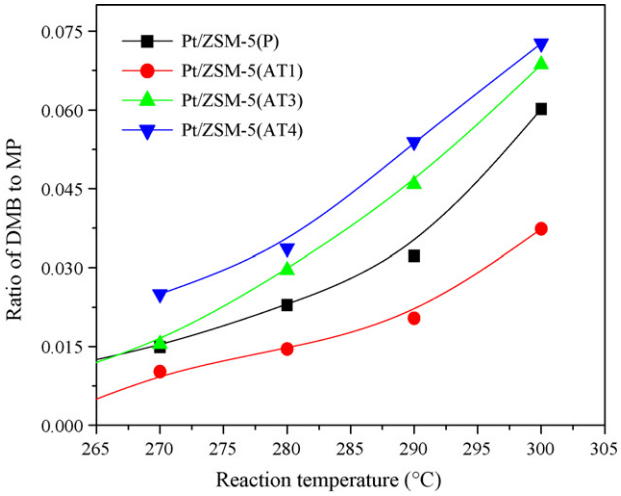

Fig. 10. Ratio of DMB to MP over Pt/ZSM-5(P) and Pt/ZSM-5(AT).

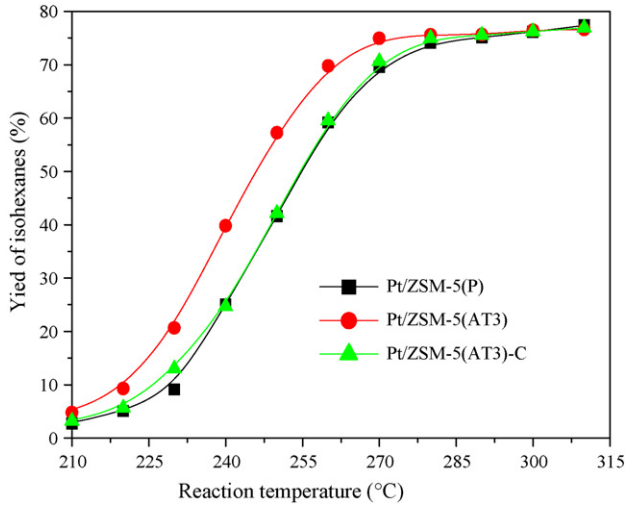

Fig. 11. Yield of isohexanes over Pt/ZSM-5(P), Pt/ZSM-5(AT3) and Pt/ZSM-5 (AT3)-C.

ization activity, but promote the formation of more multibranched isomers.

3.7. Relationship between the pore structure and acidity of ZSM-5 and isomerization performance

Generally, the strong acid sites were the active sites for n-alkane isomerization. The change in the amount of strong acid sites on the catalyst may result in the variation of *n*-alkane conversion. Pt/ZSM-5(AT1) had lower n-hexane conversion than Pt/ZSM-5(P), possibly owing to the smaller amount of strong acid sites over ZSM-5(AT1). Pt/ZSM-5(AT3) and Pt/ZSM-5(AT4) possessed the higher *n*-hexane conversion than Pt/ZSM-5(P) which may be related to the more strong acid sites over ZSM-5(AT3) and ZSM-5(AT4). Meanwhile, considerable mesopores were produced in ZSM-5(AT3) and ZSM-5(AT4). Maybe the creation of mesopores would influence the conversion. However, the selectivity for isohexanes over the different catalysts was almost equal at the same conversion of n-hexane although the different samples had different acidities and pore structures. This implied that the selectivity for isohexanes strongly depended on the conversion of n-hexane and seemed to be irrelevant to the acidity and pore structure of ZSM-5.

In order to clarify the effects of the acidity and pore structure of ZSM-5 on the isomerization activity, the yield of isohexanes on Pt/ZSM-5(P), Pt/ZSM-5(AT3) and Pt/ZSM-5(AT3)-C were compared, as shown in Fig. 11. It could be clearly seen that the yield over Pt/ZSM-5(AT3)-C was distinctly lower than the value over Pt/ZSM-5(AT3). Considering that both ZSM-5(AT3) and ZSM-5(AT3)-C possessed a large amount of mesopores while the strong acid sites over the latter were much fewer than those over the former, it could be reasonably inferred that the conversion was dependent on the strong acid sites over ZSM-5. In addition, the yield over Pt/ZSM-5(P) and Pt/ZSM-5(AT3)-C with the same amount of strong acid sites were very close although the latter had more mesopores than the former. It further confirmed that the isomerization activity was mainly dependent on the amount of the strong acid sites and irrelevant to the creation of mesopores in ZSM-5. Differently, Tromp and van Donk et al. [15,16] considered that the enhancement of isomerization activity was related to the creation of mesopores in mordenite from acid leaching. The effect of the acidity of mordenite resulting from acid-leaching on the isomerization activity was not investigated by these authors. However, the recent investigation showed that the acid leaching to mordenite resulted in the reduction of total acid sites and the increase in the strong acid sites and the enhanced isomerization activity was attributed to the increase in the strong acid sites [20], in agreement with our results. It was well-known that n-alkane in the isomerization reaction was first dehydrogenated to form the olefinic species over the metal sites, and that the olefinic species were transformed into isoalkenes over strong acid sites by skeletal isomerization and finally was hydrogenated into isoalkanes over the metal sites. The increase in the conversion with the amount of the strong acid sites suggested that the skeletal isomerization was the rate-limiting step in the isomerization of n-alkanes.

In addition, the acid properties may also influence the conversion of n-hexane. The conversion over different catalysts increased in the following order: Pt/ZSM-5(AT1) < Pt/ZSM-5(P) < Pt/ZSM-5(AT3) < Pt/ZSM-5(AT4), in agreement with the amount of the strong Brønsted acid sites over different samples, implying that the isomerizatoin reaction of n-alkanes was catalyzed by the strong Brønsted acid sites, as reported by Baburek and Nováková [45]. However, one should note that the severe alkali treatment led to a drastic increase in the strong Lewis acid sites, as well as the strong Brønsted acid sites over ZSM-5(AT4), suggesting that the higher conversion over Pt/ZSM-5(AT4) was also related to the presence of the large amount of Lewis acid sites, in line with the opinion of van Bokhoven et al. [18]. Consequently, it was reasonable to conclude that the increase in both strong Brønsted acid sites and strong Lewis acid sites was favorable to the enhancement in the conversion of n-hexane. This suggested that the conversion was dependent on the amount of strong acid sites and irrelevant to the acid properties.

In addition, the relative amounts of DMB and MP (expressed as the ratio of DMB to MP) in isomers over catalysts with different acidities and different pore structures were fairly different. First, the effect of pore structure on the relative amount of different isomers was investigated. The ratios of DMB to MP over Pt/ZSM-5(P) and Pt/ZSM-5(AT3)-C with the almost equal strong acid sties are shown in Fig. 12; the ratio over the latter was much higher than that over the former. Reasonably, the higher ratio over Pt/ZSM-5(AT3)-C should be attributed to the existence of the numerous mesopores. Besides, ZSM-5(AT3)-C possessed more mesopores than ZSM-5(AT3) by the Al_{EF} removal with acid leaching and the ratio of DMB to MP over Pt/ZSM-5(AT3)-C was further enhanced. This is also due to the fact that the presence of mesopores was favorable to the increase in the formation of DMB. However, the study from Tromp et al. [16] showed that the creation of mesopores in mordenite led to a reduction in the formation of multibranched

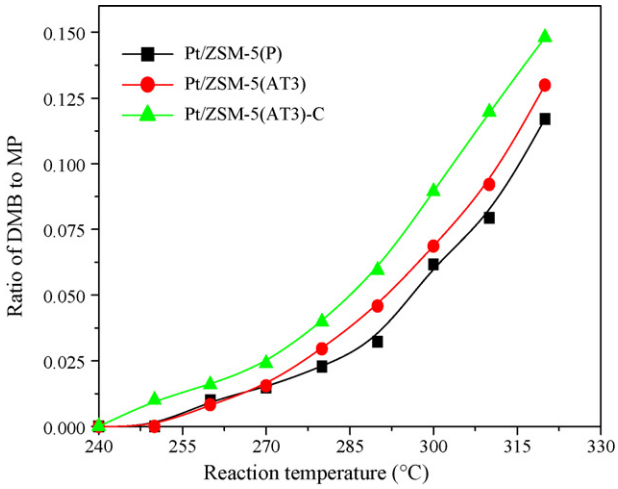

Fig. 12. The ratio of DMB to MP over Pt/ZSM-5(P), Pt/ZSM-5(AT3) and Pt/ZSM-5 (AT3)-C.

alkanes and an increase in the formation of monobranched alkanes in n-hexane isomerization, which was contrary to the present results. The discrepancy may be related to the different pore structures of the two zeolites. The pore channel of ZSM-5 was zigzag and so small as to limit the further transformation of MP to bulky molecules DMB. The formation of DMB on ZSM-5 (P) may occur at the intersections of pore channels. The creation of mesopores in ZSM-5 provided the large space for the formation of DMB and resulted in the enhanced ratio of DMB to MP in isomers.

The effect of acidity of ZSM-5 on the distribution of isomers was investigated by only changing the amount of the strong acid sites and keeping the pore structure unaltered. Although ZSM-5(AT1) had very few new mesopores, compared with ZSM-5(P), here the pore structure of the two samples was considered to be the same. The much lower ratio of DMB to MP over Pt/ZSM-5(AT1) than over Pt/ZSM-5(P) should be reasonably attributed to the fewer strong acid sites on the former. In addition, if the effect of the very few new mesopores in ZSM-5(AT1) was also considered, the lower ratio of DMB to MP over Pt/ZSM-5(AT1) was further proved to be related to the reduction in the strong acid sites because the generation of the mesopores should be more favorable to the formation of DMB. Accordingly, the relative amount of DMB and MP was also dependent on the amount of the strong acid sites except for the pore structure. On one hand, multibranched alkanes as the secondary products of n-alkanes isomerization are formed by further transformation of monobranched alkanes over strong acid sites [9,10,12]. With the reduction of the strong acid sites over ZSM-5, the further transformation of MP to DMB catalyzed by the strong acid sites would be retarded to some extent. From this point, the reduction in strong acid sites was unfavorable to the formation of DMP. On the other hand, the reduction of the strong acid sites led to the reduction in n-hexane conversion, which would lower the concentration of MP in pore channels. Thus, the rate of the conversion of MP to DMB slowed down and finally the relative amount of DMP in isomers decreased. Based on the above two sides, the relative amount of DMB and MP in isomers was related to the amount of the strong acid sites and the reduction of the strong acid sites would lead to the reduction of the formation of DMB. To sum up, the isomerization activity was influenced only by the acidity of ZSM-5 and the distribution of isohexanes was synchronously influenced by both the acidity and the pore structure of ZSM-5.

4. Conclusions

The mild alkali treatment led to the removal of extra framework Al of ZSM-5(P) and then an obvious reduction of the strong acid sites. The severe treatment led to the creation of the stronger acid sites and new mesopores, attributed to framework dealumination and desilication, respectively. The changes in the acidity and pore structure of ZSM-5 had great influences on the isomerization performance. n-Hexane conversion was dependent on the amount of strong acid sites on ZSM-5 and irrelevant to the acidic properties and pore structure, while the selectivity for isohexanes was related only to the conversion. The distribution of isomers was related to both the pore structure and the amount of the strong acid sites over ZSM-5. The relative amount of DMB in isomers increased with the creation of mesopores and the increase in the strong acid sites. Therefore, the high isomerization activity and more DMB could be obtained by the alkali treatment of ZSM-5 under the suitable conditions.

Acknowledgements

We thank the financial support of this work from Ministry of Science and Technology of China (Grant: 2004 CB 720603) and Postdoctoral Science Foundation of P.R. China (200800430081).

References

[1] J.A. Martens, P.A. Jacobs, J. Weitkamp, Appl. Catal. 20 (1986) 239–281.
[2] H.Y. Chu, M.O. Rosynek, J.H. Lunsford, J. Catal. 178 (1998) 352–362.
[3] A.D. Lucas, P. Sánchez, F. Dorado, M.J. Ramos, J.L. Valverde, Appl. Catal. A 294 (2005) 215–225.
[4] G. Boskovic, R. Micic, P. Pavlovic, P. Putanov, Catal. Today 65 (2001) 123–128.
[5] A. Lugstein, A. Jentys, H. Vinek, Appl. Catal. A 166 (1998) 29–38.
[6] R. Ravishankar, S. Sivasanker, Appl. Catal. A 42 (1996) 47–59.
[7] P. Canñizares, A.D. Lucas, F. Dorado, A. Durán, I. Asencio, Appl. Catal. A 169 (1998) 137–150.
[8] R. Roldán, F.J. Romero, C.J. Sanchidrián, J.M. Marinás, J.P. Gómez, Appl. Catal. A 288 (2005) 104–115.
[9] A. Patrigeon, E. Benazzi, C. Travers, J.Y. Bernhard, Catal. Today 65 (2001) 149–155.
[10] P. Raybaud, A. Patrieon, H. Toulhoat, J. Catal. 197 (2001) 98–112.
[11] S.M. Babitz, B.A. Williams, J.T. Miller, R.Q. Snur, W.O. Haag, H.H. Kung, Appl. Catal. A 179 (1999) 71–86.
[12] A. Soualah, J.L. Lemberton, L. Pinard, M. Chater, P. Magnoux, K. Mljord, Appl. Catal. A 336 (2008) 23–28.
[13] P. Cañizares, A.D. Lucas, F. Dorado, D. Pérez, Appl. Catal. A 190 (2000) 233–239.
[14] W.M. Zhang, P.G. Smirniotis, J. Catal. 182 (1999) 400–416.
[15] S. van Donk, A. Broersma, O.L.J. Gijzeman, J.A.V. Bokhoven, J.H. Bitter, K.P.D. Jong, J. Catal. 204 (2001) 272–280.
[16] M. Tromp, J.A.V. Bokhoven, M.T.G. Oostenbrink, J.H. Bitter, K.P.D. Jong, D.C. Koningsberger, J. Catal. 190 (2000) 209–214.
[17] R.A. Beyerlein, C.C. Feng, J.B. Hall, B.J. Huggins, G.J. Ray, Top. Catal. 4 (1997) 27–42.
[18] J.A. van Bokhoven, M. Tromp, D.C. Koningsberger, J.T. Miller, J.A.Z. Pieterse, J.A. Lercher, B.A. Williams, H.H. Kung, J. Catal. 202 (2001) 129–140.
[19] S. Gopal, P.G. Smirniotis, J. Catal. 225 (2004) 278–287.
[20] S.K. Saxena, R. Kamble, M. Singh, M.O. Garg, N. Viswanadham, Catal. Today 130 (2008) 501–508.
[21] N. Viswanadham, L. Dixit, J.K. Gupta, M.O. Garg, J. Mol. Catal. A 258 (2006) 15–21.
[22] A. Corma, A. Martínez, L.D. Fernandes, J.L.F. Monteiro, E.F. Sousa-Aguiar, Stud. Surf. Sci. Catal. 94 (1995) 456–463.
[23] S.H. Baeck, W.Y. Lee, Appl. Catal. A 168 (1998) 171–177.
[24] T. Suzuki, T. Okuhara, Micropor. Mesopor. Mater. 43 (2001) 83–89.
[25] J.C. Groen, L.A.A. Peffer, J.A. Moulijn, J.P. Ramírez, Colloids Surf. A Physicochem. Eng. Aspects 241 (2004) 53–58.
[26] G. Lietz, K.H. Schnabel, Ch. Peuker, Th. Gross, W. Storek, J. Volter, J. Catal. 148 (1994) 562–568.
[27] T. Sano, Y. Nakajima, Z.B. Wang, Y. Kawakami, K. Soga, A. Iwasakim, Micropor. Mater. 12 (1997) 71–77.
[28] M. Ogura, S.Y. Shinomiya, J. Tateno, Y. Nara, M. Nomura, E. Kikuchi, M. Matsukata, Appl. Catal. A 219 (2001) 33–43.
[29] L.L. Su, L. Liu, J.Q. Zhuang, H.X. Wang, Y.G. Li, W.J. Shen, Y.D. Xu, X.H. Bao, Catal. Lett. 91 (2003) 155–167.
[30] J.C. Groen, L.A.A. Peffer, J.A. Moulijn, J. Perez-Ramırez, Micropor. Mesopor. Mater. 69 (2004) 29–34.
[31] X.T. Wei, P.G. Smirniotis, Micropor. Mesopor. Mater. 97 (2006) 97–106.
[32] H. Matsuura, N. Katada, M. Niwa, Micropor. Mesopor. Mater. 66 (2003) 283–296.
[33] Y.Q. Song, X.X. Zhu, Y. Song, L.Y. Xu, Appl. Catal. A 302 (2006) 69–77.
[34] Y.N. Li, S.L. Liu, Z.K. Zhang, S.J. Xie, X.X. Zhu, L.Y. Xu, Appl. Catal. A 338 (2008) 100–113.
[35] R.M. Dessau, E.W. Valyocsik, N.H. Goeke, Zeolites 12 (1992) 776.
[36] R.L.V. Mao, S. Xiao, A. Ramsaran, J. Yao, J. Mater. Chem. 4 (1994) 605–610.
[37] C.S. Cundy, M.S. Henty, R.J. Plaisted, Zeolites 15 (1995) 342–352.
[38] A. Cizmek, B. Subotic, R. Aiello, F. Crea, A. Nastro, C. Tuoto, Micropor. Mater. 4 (1995) 159–168.
[39] A. Cizmek, B. Subotic, I. Smit, A. Tonejc, R. Aiello, F. Crea, A. Nastro, Micropor. Mater. 8 (1997) 159–169.
[40] M. Ogura, S. Shinomiya, J. Tateno, Y. Nara, E. Kikuchi, M. Matsukata, Chem. Lett. (2000) 882–883.
[41] B.A. Williams, S.M. Babitz, J.T. Miller, R.Q. Snurr, H.H. Kung, Appl. Catal. A 177 (1999) 161–175.
[42] E. Loeffler, Ch. Peuker, H.G. Jerschkewitz, Catal. Today 3 (1988) 415–420.
[43] C.S. Triantafillidis, A.G. Vlessidis, L. Nalbandian, N.P. Evmirids, Micropor. Mesopor. Mater. 47 (2001) 369–388.
[44] D.G. Wei, J.L. Zhou, B.J. Zhang, J. Fuel Chem. Technol. 24 (1996) 103–107.
[45] E. Baburek, J. Nováková, Appl. Catal. A 185 (1999) 123–130.